Structural Engineering and Mechanics, *Vol. 57, No. 1 (2016) 141-159*
DOI: http://dx.doi.org/10.12989/sem.2016.57.1.141

A hybrid method for dynamic stiffness identification of bearing joint of high speed spindles

Yongsheng Zhao*, Bingbing Zhang[a], Guoping An, Zhifeng Liu and Ligang Cai

Key Laboratory of advanced manufacturing technology, Beijing University of Technology, Beijing, 100124, P.R. China

(Received January 1, 2014, Revised December 14, 2015, Accepted December 15, 2015)

Abstract. Bearing joint dynamic parameter identification is crucial in modeling the high speed spindles for machining centers used to predict the stability and natural frequencies of high speed spindles. In this paper, a hybrid method is proposed to identify the dynamic stiffness of bearing joint for the high speed spindles. The hybrid method refers to the analytical approach and experimental method. The support stiffness of spindle shaft can be obtained by adopting receptance coupling substructure analysis method, which consists of series connected bearing and joint stiffness. The bearing stiffness is calculated based on the Hertz contact theory. According to the proposed series stiffness equation, the stiffness of bearing joint can be separated from the composite stiffness. Then, one can obtain the bearing joint stiffness fitting formulas and its variation law under different preload. An experimental set-up with variable preload spindle is developed and the experiment is provided for the validation of presented bearing joint stiffness identification method. The results show that the bearing joint significantly cuts down the support stiffness of the spindles, which can seriously affects the dynamic characteristic of the high speed spindles.

Keywords: bearing joint; dynamic stiffness; hybrid method; high speed spindles

1. Introduction

The spindle system is one of the most important parts of a machine tool, which directly affect the cutting stability and precision of the machine tool. The vibration-free operation of the spindle is affected by the dimensions of the spindle shaft, the stiffness and preload of bearing, as well as the bearing joints. With trends for higher precision and rotate speed, solutions to improve the dynamics properties in machining have become increasingly important (Cao and Altintas 2004). The experimental tests and theory models have been widely used to obtain the natural frequency and the amplitude frequency response (Altintas and Cao 2005, Cao and Altintas 2007, Kim and Lee 2001, Kim *et al*. 2002, Jones 1960). Most of previous reports focus on the bearing stiffness computation, which is considered as the support stiffness of the spindle system. However, the bearing stiffness can only partly contribute to the support stiffness of the spindle system. The stiffness of bearing joints should be considered in modeling the dynamic performance of the

*Corresponding author, Professor, E-mail: zys.swm@gamil.com
[a]M.E. Student, E-mail: myjxcad@sina.com

http://www.techno-press.org/?journal=sem&subpage=8 ISSN: 1225-4568 (Print), 1598-6217 (Online)

spindle system. The stiffness of bearing joint consists of two parts, the stiffness between inner ring of bearing and shaft, the stiffness between outer ring of bearing and bearing house.

According to these dynamic analysis results of spindle system, we can conclude that the support stiffness of the spindle shaft can seriously affect the dynamic performance of the high speed spindles. Most of previous reports focus on the bearing stiffness computation, which is considered as the support stiffness of the spindle system. The bearing stiffness can be computed in the different preload and paired form. DeMul *et al.* (1989) established the load deflection equations in a matrix form. Houpert (1997), Hernot *et al.* (2000) presented stiffness matrix forms for the angular contact ball bearings with five degrees of freedom that make it possible to use the finite element method to solve the coupled problems of the spindle-bearing systems. Based on Hertz contact theory, Hagiu and Gafitanu (1992) established the relationship between the bearing contact force and deformation to calculate the bearing stiffness and damping where the effect of oil film squeezing was considered. Guo and Parker (2012) presented a finite element/contact mechanics model of rolling element bearings with the focus of obtaining accurate bearing stiffness for a wide range of bearing types and parameters. Aydin *et al*. (2012) proposed a new bearing stiffness matrix (K_b) formulation by extending the prior single row theory presented by Lim and Singh (1990) and this method was used to guide the design of a new shaft-bearing system. Jiang and Mao (2010) investigated the variable preload technology systematically. They reported that the variable preload spindle gave outstanding behavior that the temperature rise at high speed was lower than that of the constant pressure preload spindle, and the dynamic stiffness at low speed range significantly increased. Li and Shin (2004) presented the effect of bearing configuration on the thermo-dynamic behavior of high speed spindles using the comprehensive dynamic thermo-mechanical model. Jeng and Gao (2001), Chen and Chen (2005) investigated the effect of bearing preload on the thermal behaviors of the spindle, and revealed that optimal preload for the lowest bearing temperature raise existed for a specified spindle speed, and the optimum preload, however, should be increased for higher operational speeds.

The stiffness of bearing joint is difficult to be acquired directly, which is affected by the assembly tolerance, preload and paired form of bearing. It is necessary to study the identification method for obtaining the stiffness of bearing joint. Recently, various identification approach have been presented to obtain the dynamic characteristic of the joints (Shamine *et al*. 1998, Yang *et al*. 2003, Majid *et al*. 2013, Rivin 2000). Based on the inverse relationship between the frequency response function matrix and the dynamic stiffness matrix of a multi-degree-of-freedom system, Mao *et al*. (2010) proposed a high-accuracy parameter identification method to recognize the dynamic model parameters of the joints, using the dynamic test data of the whole structure including the joints. Čelič and Boltežar (2009) considered the model of the joint as a coupled dynamic stiffness matrix, which generally includes six degrees of freedom (DoFs), and use a substructure synthesis method to identify the joint dynamic properties. Royston (2008) established the relationship of Iwan model to reflect the nonlinear and energy-dissipative behavior of the joints. Hamid and Mostafa (2010) employed the measured spindle-machine frequency response functions (FRFs) and analytical models of the tool and the holder to predict the tool tip FRFs for different sets of tools and holders mounted on the machine spindle without repeated experimental measurements. Hassan *et al*. (2007) identified the parameters of an assumed nonlinear joint model by force-state mapping from time-domain acceleration records in response to a single-frequency excitation close to the first natural frequency. Kashani and Nobari (2010) proposed a simple identification technique, which does not require any sophisticated measurement hardware and techniques. Michael *et al*. (2002) took into account the uncertainty and variability of the model

parameters by representing the parameters as fuzzy numbers that can be identified on the basis of the measured data. Hu *et al*. (2009) proposed an identification method of the dynamic stiffness matrix of a bearing joint region on the basis of experiments. However, they only obtained the support stiffness of the spindle shaft, which is difficult to reflect the effect of the bearing joint to the dynamic property of spindle system.

In this paper, a hybrid identification method is presented to achieve the dynamic stiffness of bearing joint for the high speed spindles. The support stiffness of spindle system is considered as series connected bearing and joint stiffness. Based on the proposed series stiffness equation, the stiffness of bearing joint can be separated from the composite stiffness. The experiment is provided for the validation of presented bearing joint identification method. The effect of bearing joint to the spindle system is analyzed, and the stiffness fitting formula and its variation law under different preloads is obtained. The results show that the bearing joint significantly cuts down the support stiffness of the spindles, which can seriously affect the dynamic performance of the high speed spindles. Therefore, the stiffness of bearing joint must be considered for obtaining the accurately dynamic characteristics of high speed spindle system.

2. Identification method of bearing joint stiffness

This section details a proposed hybrid methodology for obtaining the stiffness of bearing joint. Fig. 1 shows the logic of the formulation that is a combination of analytical and experimental method. The frequency response function of shaft and spindle system can be obtained by the FE model and excitation experiment, then the receptance coupling substructure analysis method is introduced to identify the support stiffness of spindle. The stiffness of bearing group can be computed based on the model presented by Aydin *et al*. (2012). According to the proposed series stiffness equation of spindle support system, the stiffness of bearing joint can be separated from the identified support stiffness. The following sub-sections detail individual steps in the overall process.

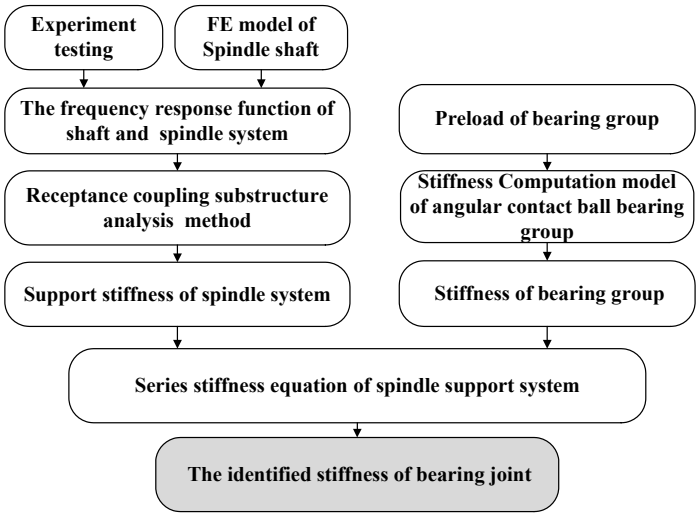

Fig. 1 Logic of the hybrid method

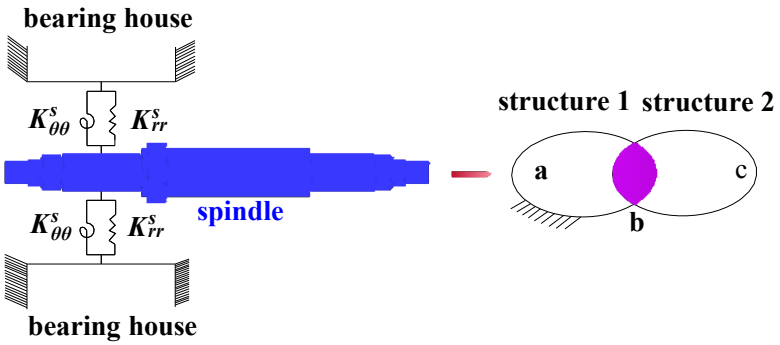

Fig. 2 Bearing house, shaft and joint stiffness

2.1 Identification of the support stiffness between the spindle-shaft and bearing house

The receptance coupling substructure analysis (RCSA) (Majid *et al*. 2013) method is adapted to identify the support stiffness of the spindle system. The basic strategy of RCSA method is to measure the FRFs of a substructure system without joints and an assembly system with joints. According to the displacement and stress constrained condition of substructures, we can obtain the dynamic equations of substructures and the assembly system. The difference between the dynamic properties of the two cases is the results of the joints (Mao *et al*. 2010). As shown in Fig. 2, the spindle system is composed of bearing house and shaft connected by the support stiffness that are assumed to be formed by radial and angular stiffness, where the K^s_{rr} is the radial support stiffness, and the $K^s_{\theta\theta}$ represents the angular support stiffness. Considering the model with three systems, region *a* and *c* represent the regions excluding the bearing and joints in bearing house and shaft respectively, and region *b* represents the region of joints which is composed of the bearing and joints.

Assuming no external moment action on the coordinates *a* and *c*, $\mathbf{m}_a^{(1)} = \mathbf{0}$, $\mathbf{m}_c^{(2)} = \mathbf{0}$, the relationship between the input and the output of the substructure 1 and 2 can be expressed as

$$\begin{Bmatrix} \mathbf{x}_a^{(1)} \\ \mathbf{x}_b^{(1)} \\ \boldsymbol{\theta}_b^{(1)} \end{Bmatrix} = \mathbf{H}^{(1)} \begin{Bmatrix} \mathbf{f}_a^{(1)} \\ \mathbf{f}_b^{(1)} \\ \mathbf{m}_b^{(1)} \end{Bmatrix} \quad \text{and} \quad \begin{Bmatrix} \mathbf{x}_c^{(2)} \\ \mathbf{x}_b^{(2)} \\ \boldsymbol{\theta}_b^{(2)} \end{Bmatrix} = \mathbf{H}^{(2)} \begin{Bmatrix} \mathbf{f}_c^{(2)} \\ \mathbf{f}_b^{(2)} \\ \mathbf{m}_b^{(2)} \end{Bmatrix} \tag{1}$$

where the **x**, **θ**, **f** and **m** are the displacement, the angular displacement, the force and moment, respectively. The superscript **(1)** and **(2)** represents the substructure 1 and 2, respectively. And the subscripts **a** and **b** are the section *a* and *b*, respectively. The $\mathbf{H}^{(1)}$ and $\mathbf{H}^{(2)}$ is the receptance matrices of the substructure 1 and 2, which can be expressed as

$$\mathbf{H}^{(1)} = \begin{bmatrix} \mathbf{TT}_{aa}^{(1)} & \mathbf{TT}_{ab}^{(1)} & \mathbf{TR}_{ab}^{(1)} \\ \mathbf{TT}_{ba}^{(1)} & \mathbf{TT}_{bb}^{(1)} & \mathbf{TR}_{bb}^{(1)} \\ \mathbf{RT}_{ba}^{(1)} & \mathbf{RT}_{bb}^{(1)} & \mathbf{RR}_{bb}^{(1)} \end{bmatrix} \quad \text{and} \quad \mathbf{H}^{(2)} = \begin{bmatrix} \mathbf{TT}_{cc}^{(2)} & \mathbf{TT}_{cb}^{(2)} & \mathbf{TR}_{cb}^{(2)} \\ \mathbf{TT}_{bc}^{(2)} & \mathbf{TT}_{bb}^{(2)} & \mathbf{TR}_{bb}^{(2)} \\ \mathbf{RT}_{bc}^{(2)} & \mathbf{RT}_{bb}^{(2)} & \mathbf{RR}_{bb}^{(2)} \end{bmatrix} \tag{2}$$

where, **TT**, **TR**, **RT** and **RR** are the frequency response matrices corresponding to the translational degrees of freedom (TDOFs) and rotational degrees of freedom (RDOFs). For the internal

coordinates *a*, only TDOFs are considered, while both TDOFs and RDOFs are considered for the joint coordinates *b* and *c*, which is denoted in the same way in Čelič and Boltežar (2009).

For region *b*, the equilibrium equations of force and torque can be expressed as

$$\mathbf{f}_{\mathrm{b}}^{(1)} + \mathbf{f}_{\mathrm{b}}^{(2)} = \mathbf{0} \quad \text{and} \quad \mathbf{m}_{\mathrm{b}}^{(1)} + \mathbf{m}_{\mathrm{b}}^{(2)} = \mathbf{0} \tag{3}$$

Then, we can obtain the dynamic equations of the joint as

$$\begin{Bmatrix} \mathbf{x}_{\mathrm{b}}^{(2)} - \mathbf{x}_{\mathrm{b}}^{(1)} \\ \boldsymbol{\theta}_{\mathrm{b}}^{(2)} - \boldsymbol{\theta}_{\mathrm{b}}^{(1)} \end{Bmatrix} = \mathbf{H}_{\mathrm{J}} \begin{Bmatrix} \mathbf{f}_{\mathrm{b}}^{(2)} \\ \mathbf{m}_{\mathrm{b}}^{(2)} \end{Bmatrix} \tag{4}$$

where, the $\mathbf{H}_{\mathrm{j}}$ is the receptance matrices of joints.

According to the Eq. (1), (2) and (3), we can obtain the equation as

$$\begin{Bmatrix} \mathbf{x}_{\mathrm{b}}^{(2)} - \mathbf{x}_{\mathrm{b}}^{(1)} \\ \boldsymbol{\theta}_{\mathrm{b}}^{(2)} - \boldsymbol{\theta}_{\mathrm{b}}^{(1)} \end{Bmatrix} = \begin{pmatrix} -\mathbf{TT}_{\mathrm{ba}}^{(1)} & \mathbf{TT}_{\mathrm{bc}}^{(2)} \\ -\mathbf{RT}_{\mathrm{ba}}^{(1)} & \mathbf{RT}_{\mathrm{bc}}^{(2)} \end{pmatrix} \begin{Bmatrix} \mathbf{f}_{\mathrm{a}}^{(1)} \\ \mathbf{f}_{\mathrm{c}}^{(2)} \end{Bmatrix} - \begin{bmatrix} \mathbf{TT}_{\mathrm{bb}}^{(1)} + \mathbf{TT}_{\mathrm{bb}}^{(2)} & \mathbf{TR}_{\mathrm{bb}}^{(1)} + \mathbf{TR}_{\mathrm{bb}}^{(2)} \\ \mathbf{RT}_{\mathrm{bb}}^{(1)} + \mathbf{RT}_{\mathrm{bb}}^{(2)} & \mathbf{RR}_{\mathrm{bb}}^{(1)} + \mathbf{RR}_{\mathrm{bb}}^{(2)} \end{bmatrix} \begin{Bmatrix} \mathbf{f}_{\mathrm{b}}^{(2)} \\ \mathbf{m}_{\mathrm{b}}^{(2)} \end{Bmatrix} \tag{5}$$

Substituting the Eq. (4) into Eq. (5), the following equation can be deduced in the form

$$\begin{Bmatrix} \mathbf{f}_{\mathrm{b}}^{(2)} \\ \mathbf{m}_{\mathrm{b}}^{(2)} \end{Bmatrix} = \mathbf{H}_{\mathrm{B}}^{-1} \begin{bmatrix} -\mathbf{TT}_{\mathrm{ba}}^{(1)} & \mathbf{TT}_{\mathrm{bc}}^{(2)} \\ -\mathbf{RT}_{\mathrm{ba}}^{(1)} & \mathbf{RT}_{\mathrm{bc}}^{(2)} \end{bmatrix} \begin{Bmatrix} \mathbf{f}_{\mathrm{a}}^{(1)} \\ \mathbf{f}_{\mathrm{c}}^{(2)} \end{Bmatrix} \tag{6}$$

where

$$\mathbf{H}_{\mathrm{B}} = \mathbf{H}_{\mathrm{J}} + \begin{bmatrix} \mathbf{TT}_{\mathrm{bb}}^{(1)} + \mathbf{TT}_{\mathrm{bb}}^{(2)} & \mathbf{TR}_{\mathrm{bb}}^{(1)} + \mathbf{TR}_{\mathrm{bb}}^{(2)} \\ \mathbf{RT}_{\mathrm{bb}}^{(1)} + \mathbf{RT}_{\mathrm{bb}}^{(2)} & \mathbf{RR}_{\mathrm{bb}}^{(1)} + \mathbf{RR}_{\mathrm{bb}}^{(2)} \end{bmatrix} \tag{7}$$

For the assembles of spindle and bearing house, the relationship of force and response can be expressed as

$$\begin{Bmatrix} \mathbf{x}_{\mathrm{a}}^{(1)} \\ \mathbf{x}_{\mathrm{c}}^{(2)} \end{Bmatrix} = \mathbf{H}^{\mathrm{w}} \begin{Bmatrix} \mathbf{f}_{\mathrm{a}}^{(1)} \\ \mathbf{f}_{\mathrm{c}}^{(2)} \end{Bmatrix} \tag{8}$$

where, $\mathbf{H}^{\mathrm{w}}$ is the receptance matrices of assembles. Rearrange the Eq. (1) and (2), the $\mathbf{x}_{\mathrm{a}}^{(1)}$, $\mathbf{x}_{\mathrm{c}}^{(2)}$ can be written in the form

$$\begin{Bmatrix} \mathbf{x}_{\mathrm{a}}^{(1)} \\ \mathbf{x}_{\mathrm{c}}^{(2)} \end{Bmatrix} = \begin{bmatrix} \mathbf{TT}_{\mathrm{aa}}^{(1)} & \mathbf{0} \\ \mathbf{0} & \mathbf{TT}_{\mathrm{cc}}^{(2)} \end{bmatrix} \begin{Bmatrix} \mathbf{f}_{\mathrm{a}}^{(1)} \\ \mathbf{f}_{\mathrm{c}}^{(2)} \end{Bmatrix} + \begin{bmatrix} \mathbf{TT}_{\mathrm{ab}}^{(1)} & \mathbf{TR}_{\mathrm{ab}}^{(1)} \\ -\mathbf{TT}_{\mathrm{cb}}^{(2)} & -\mathbf{TR}_{\mathrm{cb}}^{(2)} \end{bmatrix} \begin{Bmatrix} \mathbf{f}_{\mathrm{b}}^{(2)} \\ \mathbf{m}_{\mathrm{b}}^{(2)} \end{Bmatrix} \tag{9}$$

Substituting the joint's characteristics (6) into Eq. (9), the following equation is obtained

$$\begin{Bmatrix} \mathbf{x}_{\mathrm{a}}^{(1)} \\ \mathbf{x}_{\mathrm{c}}^{(2)} \end{Bmatrix} = \left(\begin{bmatrix} \mathbf{TT}_{\mathrm{aa}}^{(1)} & \mathbf{0} \\ \mathbf{0} & \mathbf{TT}_{\mathrm{cc}}^{(2)} \end{bmatrix} + \begin{bmatrix} \mathbf{TT}_{\mathrm{ab}}^{(1)} & \mathbf{TR}_{\mathrm{ab}}^{(1)} \\ -\mathbf{TT}_{\mathrm{cb}}^{(2)} & -\mathbf{TR}_{\mathrm{cb}}^{(2)} \end{bmatrix} \mathbf{H}_{\mathrm{B}}^{-1} \begin{bmatrix} -\mathbf{TT}_{\mathrm{ba}}^{(1)} & \mathbf{TT}_{\mathrm{bc}}^{(2)} \\ -\mathbf{RT}_{\mathrm{ba}}^{(1)} & \mathbf{RT}_{\mathrm{bc}}^{(2)} \end{bmatrix} \right) \begin{Bmatrix} \mathbf{f}_{\mathrm{a}}^{(1)} \\ \mathbf{f}_{\mathrm{c}}^{(2)} \end{Bmatrix} \tag{10}$$

According to Eq. (8) and (10), the receptance matrices of assembles $\mathbf{H}^{\mathrm{w}}$ can be written in the form

$$\mathbf{H}^{\mathrm{w}} = \begin{bmatrix} \mathbf{TT}_{\mathrm{aa}}^{1} & \mathbf{0} \\ \mathbf{0} & \mathbf{TT}_{\mathrm{cc}}^{2} \end{bmatrix} + \begin{bmatrix} \mathbf{TT}_{\mathrm{ab}}^{1} & \mathbf{TR}_{\mathrm{ab}}^{1} \\ -\mathbf{TT}_{\mathrm{cb}}^{2} & -\mathbf{TR}_{\mathrm{cb}}^{2} \end{bmatrix} \mathbf{H}_{\mathrm{B}}^{-1} \begin{bmatrix} -\mathbf{TT}_{\mathrm{ba}}^{1} & \mathbf{TT}_{\mathrm{bc}}^{2} \\ -\mathbf{RT}_{\mathrm{ba}}^{1} & \mathbf{RT}_{\mathrm{bc}}^{2} \end{bmatrix} \tag{11}$$

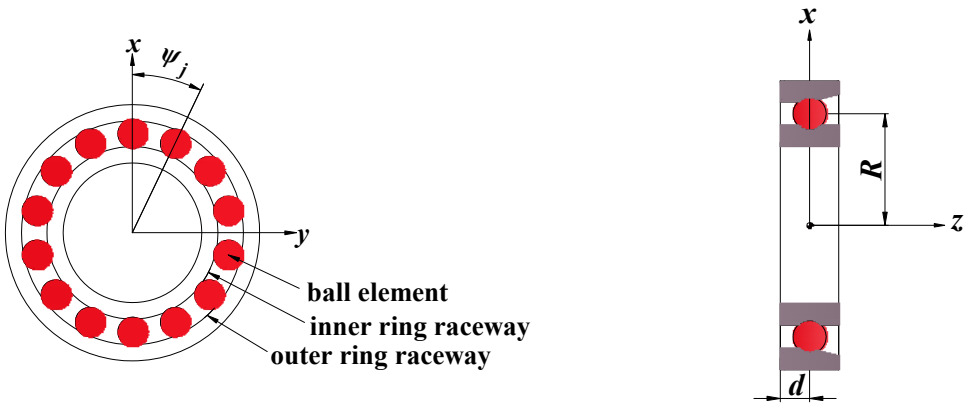

(a) Axial view (b) Radial view

Fig. 3 Schematic diagram of angular contact ball bearing

For the assemble of spindle system, the bearing house is fixed in the test table. Therefore, the receptance matrices of the substructure 1 are defined by $\mathbf{H}^{(1)}=\mathbf{0}$. The Eq. (7) and (11) can be simplified in the following form

$$\hat{\mathbf{H}}_{\mathrm{B}} = \mathbf{H}_{\mathrm{J}} + \begin{bmatrix} \mathbf{TT}_{\mathrm{bb}}^{2} & \mathbf{TR}_{\mathrm{bb}}^{2} \\ \mathbf{RT}_{\mathrm{bb}}^{2} & \mathbf{RR}_{\mathrm{bb}}^{2} \end{bmatrix} \tag{12}$$

$$\mathbf{TT}_{\mathrm{cc}}^{\mathrm{w}} - \mathbf{TT}_{\mathrm{cc}}^{2} = \begin{Bmatrix} -\mathbf{TT}_{\mathrm{cb}}^{2} & -\mathbf{TR}_{\mathrm{cb}}^{2} \end{Bmatrix} \hat{\mathbf{H}}_{\mathrm{B}}^{-1} \begin{Bmatrix} \mathbf{TT}_{\mathrm{bc}}^{2} \\ \mathbf{RT}_{\mathrm{bc}}^{2} \end{Bmatrix} \tag{13}$$

Finally, substituting Eq. (12) into Eq. (13) yields the simplified identification equations of spindle shaft.

$$\mathbf{H}_{\mathrm{J}} = \begin{Bmatrix} \mathbf{TT}_{\mathrm{bc}}^{2} \\ \mathbf{RT}_{\mathrm{bc}}^{2} \end{Bmatrix} \left(\mathbf{TT}_{\mathrm{cc}}^{\mathrm{w}} - \mathbf{TT}_{\mathrm{cc}}^{2} \right)^{-1} \begin{Bmatrix} -\mathbf{TT}_{\mathrm{cb}}^{2} & -\mathbf{TR}_{\mathrm{cb}}^{2} \end{Bmatrix} - \begin{bmatrix} \mathbf{TT}_{\mathrm{bb}}^{2} & \mathbf{TR}_{\mathrm{bb}}^{2} \\ \mathbf{RT}_{\mathrm{bb}}^{2} & \mathbf{RR}_{\mathrm{bb}}^{2} \end{bmatrix} \tag{14}$$

The support stiffness matrix can be expressed as

$$\mathbf{P}_{\mathrm{J}} = \mathbf{H}_{\mathrm{J}}^{-1} \tag{15}$$

Usually, the mass of joint is ignored during the identification process, only the stiffness and damping are considered. The stiffness and damping elements are used to represented the dynamic characteristics, which can be expressed as

$$\mathbf{P}_{\mathrm{J}} = \begin{bmatrix} K_{rr}^{s} + i\omega C_{rr}^{s} & K_{\theta r}^{s} + i\omega C_{\theta r}^{s} \\ K_{r\theta}^{s} + i\omega C_{r\theta}^{s} & K_{\theta\theta}^{s} + i\omega C_{\theta\theta}^{s} \end{bmatrix} = \begin{bmatrix} K_{rr}^{s} & K_{\theta r}^{s} \\ K_{r\theta}^{s} & K_{\theta\theta}^{s} \end{bmatrix} + i\omega \begin{bmatrix} C_{rr}^{s} & C_{\theta r}^{s} \\ C_{r\theta}^{s} & C_{\theta\theta}^{s} \end{bmatrix} \tag{16}$$

where, K_{rr}^{s} , C_{rr}^{s} denotes the stiffness and damping of translation-to-force, respectively. $K_{\theta r}^{s}$ and $C_{\theta r}^{s}$ are the stiffness and damping of translation-to-moment, $K_{r\theta}^{s}$ and $C_{r\theta}^{s}$ are the stiffness and damping of rotation-to-force, and $K_{\theta\theta}^{s}$, $C_{\theta\theta}^{s}$ denote the stiffness and damping of rotation-to-moment. According to results in Hamid and Mostafa (2010), the elements $K_{\theta r}^{s}$ and $K_{r\theta}^{s}$ have less effect on the dynamic behavior of the spindle assembly. Therefore, $K_{\theta r}^{s}$ and $K_{r\theta}^{s}$ can be

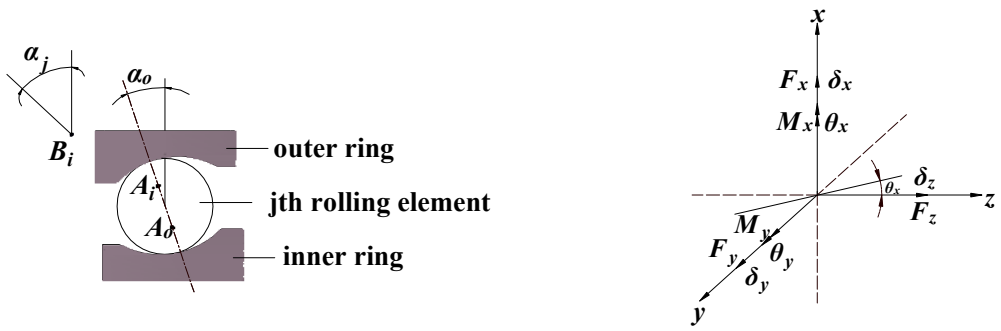

(a) Elastic deformation of a rolling element under load (b) The coordinate graph of bearing force

Fig. 4 The relationship of load and displacement for the bearing group

neglected for the purpose of improving the computational efficiency.

2.2 The stiffness computation of angular contact ball bearing group

The bearing is the critical support part for the high speed spindle system. Usually, they are used in multirow configuration form and constant preload. The bearing stiffness is a global representation of the bearing kinematic and elastic characteristics, which combines the effects of each rolling element of multi-row bearings and their interactions. In this paper, the model presented by Aydin *et al.* (2012) is adapted to compute the stiffness of angular contact ball bearing group. The angular contact ball bearing is used to support the spindle shaft. The schematic diagram is shown in Fig. 3 (a) and (b). ψ_j is the position angle of the ball element, the subscript j denotes the jth ball element. d is the axial distance between the geometric center of the bearing and the ith bearing row, R is the pitch radius.

The outer ring raceway is assumed fixed to analyze the relationship of load and displacement for the bearing group, as shown in Fig. 4 (a) and (b). A_i is the inner raceway curvature center of the unloaded rolling element, and A_o is the outer raceway curvature center of the unloaded rolling element. B_i is the inner raceway curvature center of the loaded rolling element, α_o is the unloaded contact angle, α_j is the loaded contact angle, and subscript j is the number of balls.

The relationships between the mean bearing load vector and force of bearing group in x, y, z direction/torque in x, y axis are derived based on the Hertz contact theory (Aydin *et al*. 2012).

$$\begin{cases} F_x = \sum_{i=1}^{m}\sum_{j=1}^{n} Q_j^i \cos\left(\alpha_j^i\right)\cos\left(\psi_j^i\right) \\ F_y = \sum_{i=1}^{m}\sum_{j=1}^{n} Q_j^i \cos\left(\alpha_j^i\right)\sin\left(\psi_j^i\right) \\ F_z = \sum_{i=1}^{m}\sum_{j=1}^{n} Q_j^i \sin\left(\alpha_j^i\right) \\ M_x = \sum_{i=1}^{m}\sum_{j=1}^{n} Q_j^i \left[\mathrm{R}\sin\left(\alpha_j^i\right) - \mu^i d_z^i \cos\left(\alpha_j^i\right)\right]\sin\left(\psi_j^i\right) \\ M_y = \sum_{i=1}^{m}\sum_{j=1}^{n} Q_j^i \left[-\mathrm{R}\sin\left(\alpha_j^i\right) + \mu^i d_z^i \cos\left(\alpha_j^i\right)\right]\cos\left(\psi_j^i\right) \end{cases} \tag{17}$$

where, F_x, F_y, F_z, M_x, M_y are the force of bearing in x, y, z direction, and torque in x, y axis, respectively. m is the row number of the bearing group, n is the rolling number of bearing in one row, α_j^i is the loaded contact angle (i, j is the row and rolling element indices), ψ_j^i is the angular position of the rolling element, μ is a dimensionless constant determined by the position of bearing. Q_j^i is the normal load on the element, d_z^i is the axial distance between the geometric center of the bearing and ith bearing row.

The relationship of force and displacement between the outer ring raceway and rolling element is nonlinear in the spindle-bearing system. To obtain the stiffness of bearing group, it is necessary to differentiate load in the displacement direction for obtaining the linear equations. The matrix equation between the mean bearing load vector and mean displacement vector can be rewritten as

$$\begin{Bmatrix} F_x \\ F_y \\ F_z \\ M_x \\ M_y \end{Bmatrix} = \begin{bmatrix} k_{xx} & k_{xy} & k_{xz} & k_{x\theta_x} & k_{x\theta_y} \\ & k_{yy} & k_{yz} & k_{y\theta_x} & k_{y\theta_y} \\ & & k_{zz} & k_{z\theta_x} & k_{z\theta_y} \\ & & & k_{\theta_x\theta_x} & k_{\theta_x\theta_y} \\ sym & & & & k_{\theta_y\theta_y} \end{bmatrix} \begin{Bmatrix} \delta_x \\ \delta_y \\ \delta_z \\ \theta_x \\ \theta_y \end{Bmatrix} \tag{18}$$

where, δ_x, δ_y, δ_z, θ_x, θ_y are the displacement of bearing in x, y, z direction, and rotation angle in x, y axis, respectively. $k_{xx} = \dfrac{\partial F_x}{\partial x}$, $k_{yy} = \dfrac{\partial F_y}{\partial y}$ is the radial stiffness of the bearing group in x and y direction, respectively. $k_{zz} = \dfrac{\partial F_z}{\partial z}$ is the axial stiffness of the bearing group. $k_{\theta_x\theta_x} = \dfrac{\partial M_x}{\partial \theta_x}$, $k_{\theta_y\theta_y} = \dfrac{\partial M_y}{\partial \theta_x}$ is the angular stiffness of bearing group in x, y axis, respectively. The elements except the main diagonals can be obtained by adapting the same method. For the purpose of discussion, the radial stiffness K_{xx}, K_{yy} and angular stiffness $K_{\theta_x\theta_x}$, $K_{\theta_y\theta_y}$ are replaced by the K_{br} and $K_{b\theta}$, respectively.

The Eq. (17) can be rewritten as

$$\begin{cases} F_x - \sum_{i=1}^{3}\sum_{j=1}^{14} Q_j^i \cos\left(\alpha_j^i\right)\cos\left(\psi_j^i\right) = 0 \\ F_y - \sum_{i=1}^{3}\sum_{j=1}^{14} Q_j^i \cos\left(\alpha_j^i\right)\sin\left(\psi_j^i\right) = 0 \\ F_z - \sum_{i=1}^{3}\sum_{j=1}^{14} Q_j^i \sin\left(\alpha_j^i\right) = 0 \\ M_x - \sum_{i=1}^{3}\sum_{j=1}^{14} Q_j^i \left[\mathrm{R}\sin\left(\alpha_j^i\right) - \mu^i d_z^i \cos\left(\alpha_j^i\right)\right]\sin\left(\psi_j^i\right) = 0 \\ M_y - \sum_{i=1}^{3}\sum_{j=1}^{14} Q_j^i \left[-\mathrm{R}\sin\left(\alpha_j^i\right) + \mu^i d_z^i \cos\left(\alpha_j^i\right)\right]\cos\left(\psi_j^i\right) = 0 \end{cases} \tag{19}$$

Assuming the load F_x, F_y, F_z, M_x, M_y are given, the Eq. (19) is a nonlinear equations about the unknown variables δ_x, δ_y, δ_z, θ_x and θ_y. The Newton-Raphson method is used to solve the

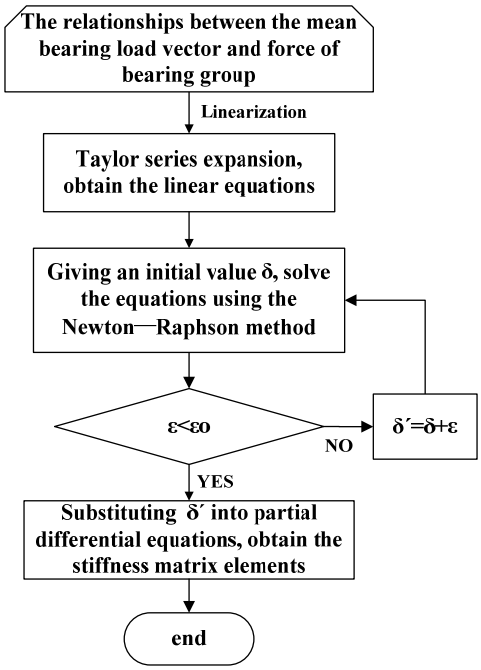

Fig. 5 The calculation flow chart for the stiffness of bearing group

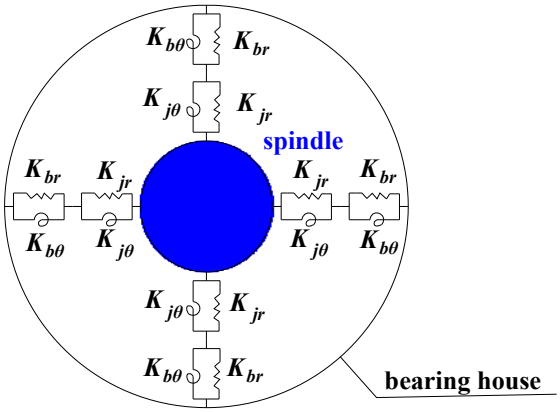

Fig. 6 The section diagram of support stiffness for the spindle system

equations. The stiffness of bearing group can be solved by adapting the following calculation flow chart.

2.3 Stiffness identification of bearing joint

In Refs (Cao and Altintas 2004, Altintas and Cao 2005, Cao and Altintas 2007, Kim and Lee 2001, Kim *et al*. 2002), the support stiffness of spindle system is determined by the bearing stiffness. However, the bearing joint stiffness should not be ignored, which can cut down the support stiffness of spindle system. The bearing stiffness of spindle can be affected by the

assembly relationship, preload and paired form of bearing. Therefore, it is necessary to identify the bearing joint stiffness and analyze the effect of the bearing joint. In this paper, the support stiffness of the spindle system is assumed to be consisted of bearing stiffness and bearing joint stiffness, which is connected in series form, as shown in Fig. 6. The stiffness of bearing joint consists of two parts, the stiffness between inner ring of bearing and shaft, the stiffness between outer ring of bearing and bearing house. For the purpose of simplified calculation, the stiffness of bearing joint is considered as a comprehensive stiffness. The section diagram of support stiffness for the spindle system is shown in Fig. 6.

The bearing is connected to the bearing joint in series to support the spindle shaft, and the series stiffness equation can be obtained as

$$\begin{cases} \dfrac{1}{K_{br}} + \dfrac{1}{K_{jr}} = \dfrac{1}{K_{rr}^{s}} \\ \dfrac{1}{K_{b\theta}} + \dfrac{1}{K_{j\theta}} = \dfrac{1}{K_{\theta\theta}^{s}} \end{cases} \tag{20}$$

where, K_{jr} and $K_{j\theta}$ are the radial and angular stiffness of bearing joint, respectively. The support stiffness K_{rr}^{s} and $K_{\theta\theta}^{s}$ of spindle system can be obtained by identification theory, as shown in Section 2.1. And the bearing stiffness K_{br}, $K_{b\theta}$ are computed by adapting the method presented by Aydin *et al.* (2012), which is described in Section 2.2. Then, the identification equation of bearing joint stiffness can be rewritten as

$$\begin{cases} K_{jr} = \dfrac{K_{rr}^{s} K_{br}}{K_{br} - K_{rr}^{s}} \\ K_{j\theta} = \dfrac{K_{\theta\theta}^{s} K_{b\theta}}{K_{b\theta} - K_{\theta\theta}^{s}} \end{cases} \tag{21}$$

3. The experimental set-up and validation of the bearing joints

The spindle system is consisted of dozens of parts, which can affect the identification precision of bearing joint. In order to validate the identification method and obtain the dynamic law under different preloads and bearing paired form, a simplified experimental set-up is designed to obtain the ideal dynamic response data as show in Fig. 7. The multi-diameter shaft with the length 707mm is designed as the spindle shaft. The dimensions and tolerances between the inner ring of the bearing and the shaft is $\varnothing$60(H7/n6) mm, which belong to the basic shaft system and interference fit. Corresponding to the dimensions and tolerances between outer ring of the bearing and bearing house is $\varnothing$110(H7/h6) mm, which is the basic hole system and clearance fit. The dimensions of multi-diameter shaft are marked in Fig. 7. The BK2F type force sensor is used to measure the preload of bearing group, and preload can be adjusted by rotating the left end of preload nut. The max number of bearing group is four for the experimental set-up. The type of angular contact ball bearing is 7212C/P2 and the parameters are shown in Table1.

As shown in Fig. 8(a) and (b), a modal testing is performed on the spindle and spindle-bearing assembly system, respectively. The piezoelectric impact hammer and PCB accelerometer is used to generate exciting forces and obtain vibration response data. The testing data is processed by the

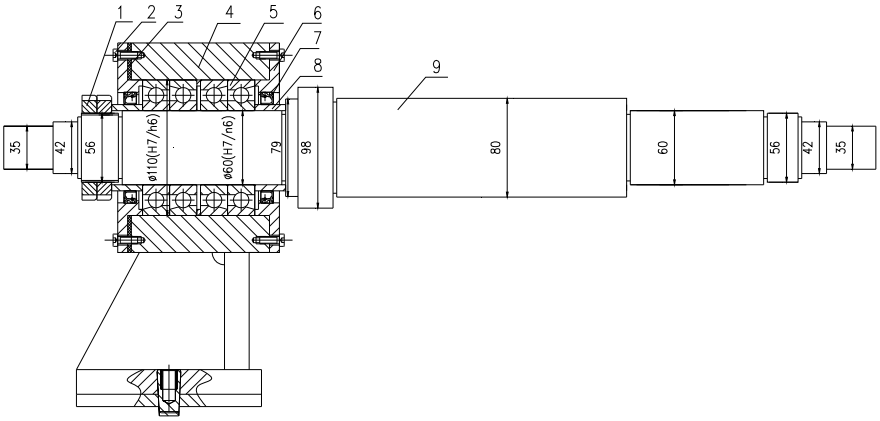

1. Preload nut 2. screw 3. washer 4. bearing house 5. angular contact ball bearing 6. positioning end cap 7. sealing ring 8. bushing 9. spindle shaft

Fig. 7 The bearing joint experimental set-up

Table 1 Parameters of the angular contact ball bearing 7212C/P2

Parameter name	Parameter values (mm)	Parameter name	Parameter values (mm)
Nominal inside ring diameter (d_i^n)	60	The unloaded contact angle (α_o)	15°
Nominal outside ring diameter (d_o^n)	110	The diameter of rolling element (D)	15.875
The curvature radius of inside groove of bearing (r_i)	8.176	The diameter of inside groove (d_i)	69.109
The curvature radius of outer groove of bearing (r_o)	8.334	The diameter of outer groove (d_o)	100.902
The number of rolling element (n)	14	Nominal width (d)	22

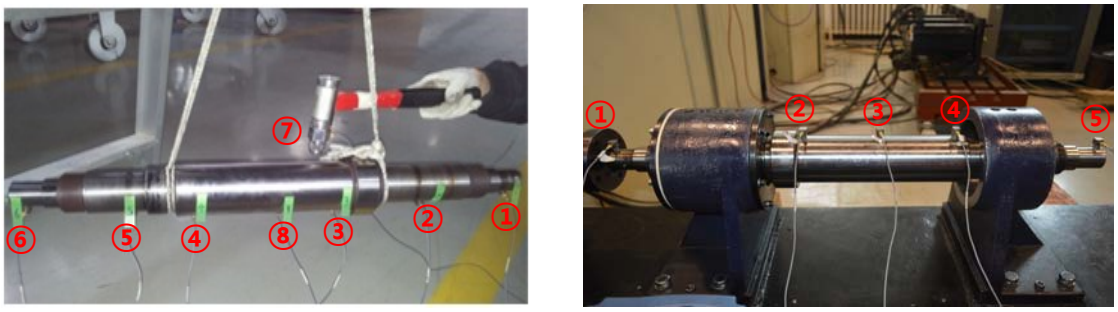

(a) Spindle shaft measurement (b) Spindle shaft-bearing assembly measurement

Fig. 8 FRF measurement using impact hammer

LMS Test.lab vibration testing and analysis system. In Fig. 8(a), ⑦ is the exciting location, ①, ②, ③, ⑧, ④, ⑤, ⑥ are the vibration pick-up points, which are distributed in the end and different cross sections of spindle for obtaining the mode of vibration. The similar measurement method is adapted to obtain the FRF of spindle shaft-bearing assembly, as in Fig. 8(b).

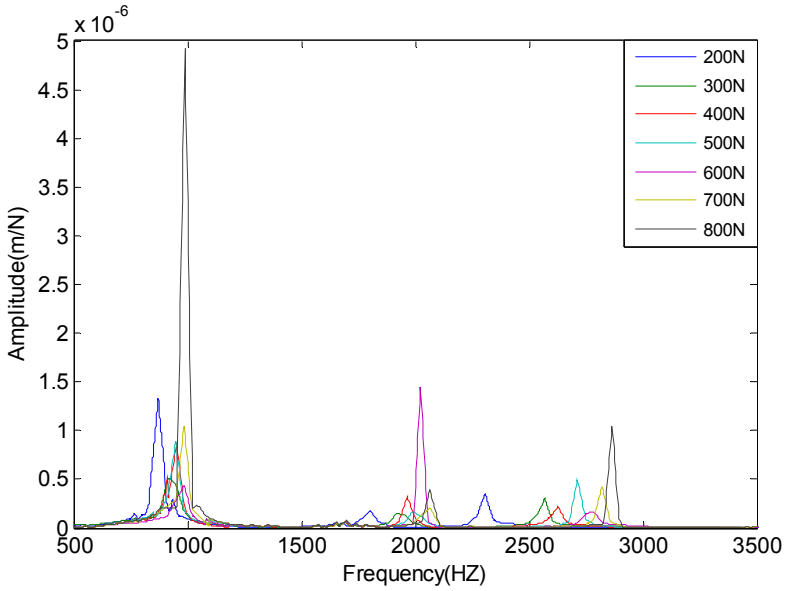

Fig. 9 The series of FRF $\mathbf{TT}_{cc}^{w}$ under four different preloads

Table 2 Natural frequencies of the assembly system under different preloads

Order	200N	300N	400N	500N	600N	700N	800N	change ratio
1	887	940	964	968	987	1001	1012	6.0%
2	1823	1934	1976	2008	2044	2074	2096	6.1%
3	2339	2597	2676	2742	2814	2862	2904	11.0%

By the hammering test, a series of acceleration FRFs can be obtained by applying 200N, 300N, 400N, 500N, 600N, 700N and 800N preload for the spindle-bearing assembly system with four row angular contact ball bearing group independently, where the back to back configuration is used for the bearing group. Fig. 9 shows the series curve $\mathbf{TT}_{cc}^{w}$, which denotes translational-to-force FRF of the spindle-bearing assembly. The natural frequencies are listed in Table 2. Comparing the natural frequencies under four different preloads, the third order is the most sensitive one to the preload change with the highest changing ratio 11.0%. Therefore, the third order's natural frequency and amplitude value are selected as inputs of identification model to obtain the support stiffness of spindle-bearing system based on the sensitivity analysis theory (Schmitz and Smith 2009). The support stiffness varies with different preloads of bearing group. However, the identification methods are generally the same.

According to the identification method, the support stiffness of spindle shaft can be obtained as shown in Table 3. The stiffness of bearing group is calculated based on the computation model of angular contact ball bearing group described in Section 2.2, as shown in Table 4. According to the proposed series stiffness equation of spindle-bearing assembly system, the stiffness of bearing joint can be obtained in different preloads, as shown in Table 5. The support stiffness is seriously cut down by the bearing joint through these bearing stiffness values. For example, the stiffness reduces from 1.34×10^{9} N/m to 4.69×10^{8} N/m for radial stiffness, and from 1.04×10^{6} N·m/rad to

Table 3 The support stiffness of spindle shaft

Preload (N)	200	300	400	500	600	700	800
Radial stiffness (N/m)	3.51×10^8	4.02×10^8	4.41×10^8	4.69×10^8	4.80×10^8	4.85×10^8	4.90×10^8
Angular stiffness (N·m/rad)	3.64×10^5	3.95×10^5	4.20×10^5	4.39×10^5	4.55×10^5	4.67×10^5	4.76×10^5

Table 4 The stiffness of bearing group

Preload (N)	200	300	400	500	600	700	800
Radial stiffness (N/m)	1.17×10^9	1.21×10^9	1.28×10^9	1.34×10^9	1.38×10^9	1.41×10^9	1.45×10^9
Angular stiffness (N·m/rad)	8.23×10^5	8.94×10^5	9.74×10^5	1.04×10^6	1.11×10^6	1.17×10^6	1.22×10^6

Table 5 The stiffness of bearing joint

Preload (N)	200	300	400	500	600	700	800
Radial stiffness (N/m)	5.01×10^8	6.02×10^8	6.73×10^8	7.22×10^8	7.36×10^8	7.39×10^8	7.40×10^8
Angular stiffness (N·m/rad)	6.53×10^5	7.08×10^5	7.38×10^5	7.60×10^5	7.71×10^5	7.77×10^5	7.81×10^5

4.39×10^5 N·m/rad for angular stiffness in the 500N preload. The reducing ratio of radial and angular stiffness are 65% and 57.8%, respectively. The results show that the bearing joint can cut down the stiffness of the support stiffness of the spindle system. However, the support stiffness can be improved by increasing the preload. The stiffness of the bearing joint can be increased by adjusting the matching relation between the bearing and shaft, bearing house, as shown in Jiang and Mao (2010), Li and Shin (2004), Jeng and Gao (2001), Chen and Chen (2005), Shamine *et al*. (1998). Therefore, it is necessary to take the stiffness of bearing joint into account for obtaining the accurate dynamic characteristic during the process of modeling the spindle system.

In order to validate the presented identification method, the spindle system model with joint stiffness is built under the 500N preload. The ANSYS software is adopted to build the spindle FE model, and the stiffness is assigned to the Matrix27 elements, which is used to connect the spindle and bearing house, as shown in Fig. 10. The modal and harmonic response analyses of spindle system are carried out to obtain the nature frequency and frequency response function, respectively. The 1st-3rd natural frequencies of spindle system are listed in Table 6. Fig. 11 shows the translation-to-force FRF $\mathbf{TT}_{cc}^{w}$. Comparing the experiment and simulation results, the errors are 2.6%, 1.4% and 1.7%, respectively. The maximum error is the 1st order nature frequency. The main reason of errors is the simplification of the multi-diameter, taper and thread during the process of the FE model simulation. As a result, the mass of spindle is increased and stiffness remains unchanged, which will make the nature frequencies smaller. In addition, the test environment, chaos of exciting force and sensor sensitivity also affect the accuracy of measurement results. However, The results show that it is valid for the presented identification method for the stiffness of bearing joint, which can be used to model the accurately spindle system.

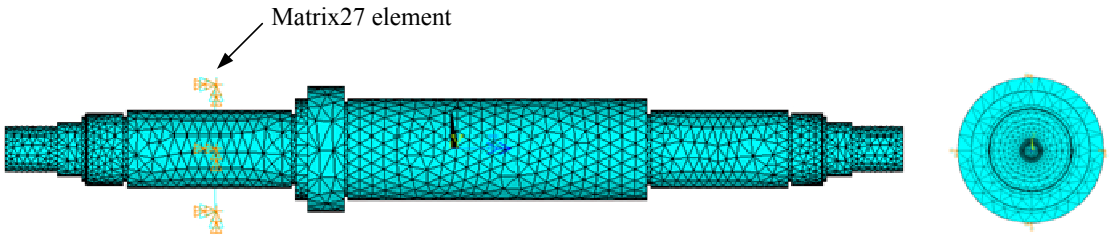

Fig. 10 The FE model of spindle system

Table 6 Natural frequencies of experiment and simulation

Preload		1st order	2nd order	3rd order
500 N	Test values	964	1976	2676
	Simulation values	940	1948	2632
	Errors	2.6%	1.4%	1.7%

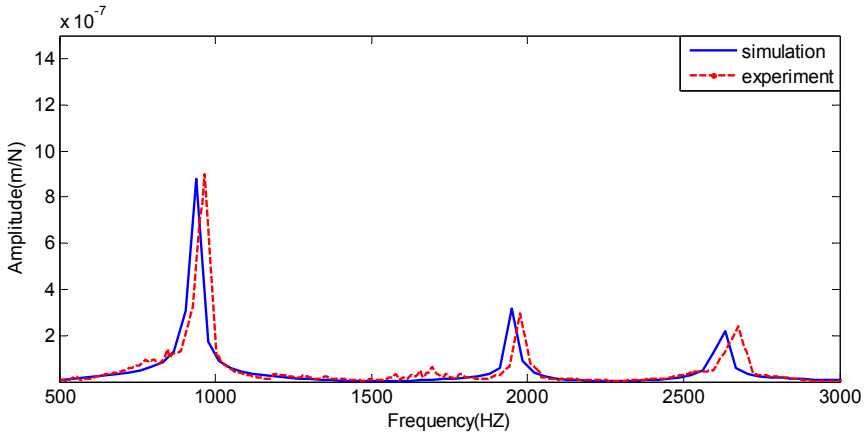

Fig. 11 The translation-to-force FRF $\mathbf{TT}_{cc}^{w}$ of experiment and simulation

4. The effect of bearing joint stiffness on the spindle system

4.1 The effect of preloads on the bearing joint stiffness

The bearing joint stiffness is mainly affected by the assembly relationship between bearing group and the spindle shaft, bearing house. However, it can also change with adjusting the preload of bearing group. The bearing joint stiffness under different preloads is shown in Fig. 12. The support radial stiffness of spindle system k_{rr}^{s}, the bearing radial stiffness k_{br} and the bearing joint radial stiffness k_{jr} are all increased with the preload increase. The bearing joint stiffness increases significantly from light preload (200N) to medium preload (500 N), in which the radial stiffness of bearing joint increases from 5.01×10^{8} N/m to 7.22×10^{8} N/m. The increase percentage is 44.1%. When the preload is larger than the medium preload, the increase rate for the bearing joint stiffness is small shown in Fig. 12(a), which indicates that it is difficult to obtain the higher support

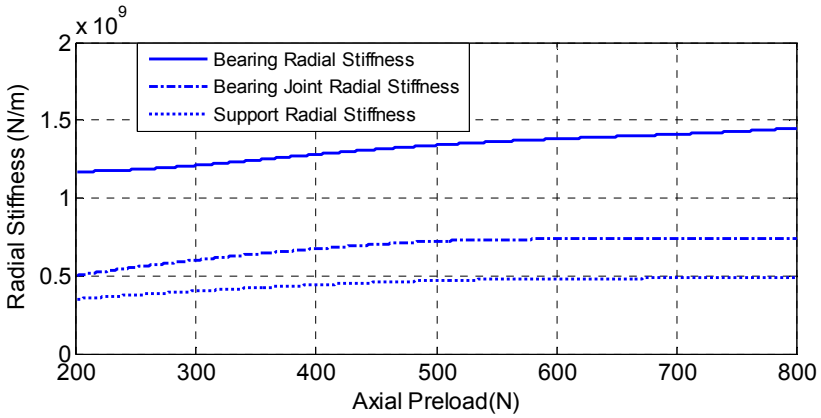

(a) The radial stiffness of bearing joint

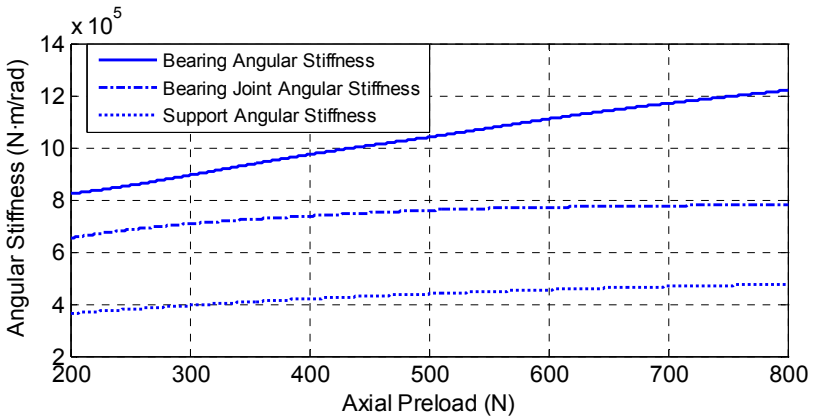

(b) The angular stiffness of bearing joint

Fig. 12 The stiffness of bearing joint under different preload

stiffness by the preload increment. In this case, the only way of increasing bearing joint stiffness is to change the fitting relationship between the bearing group and shaft, bearing house. It has similar pattern for the angular stiffness of bearing joint, as shown in Fig. 12(b). According to the analysis results, the support stiffness of spindle system is greatly reduced due to the existence of bearing joint.

In order to conveniently analyze the dynamic characteristic of spindle system, it is necessary to obtain the stiffness of bearing joint under different preload rapidly. Therefore, a fitting polynomial formula is developed according to the analytic results of bearing joint. Three multi-form fitting formulae can be established for the radial and angular stiffness of bearing joint. The fitting curve of bearing joint stiffness is shown in Fig. 13.

$$K_{jr} = 1.1x^3 - 2708x^2 + 2.2\times10^6 x + 1.6\times10^8 \tag{22}$$

$$K_{j\theta} = 0.0007x^3 - 1.6x^2 + 1162x + 4.8\times10^5 \tag{23}$$

where, x is the preload of bearing group. However, the presented fitting polynomial formulas are only effective for the established experimental condition. It is necessary to identify the bearing

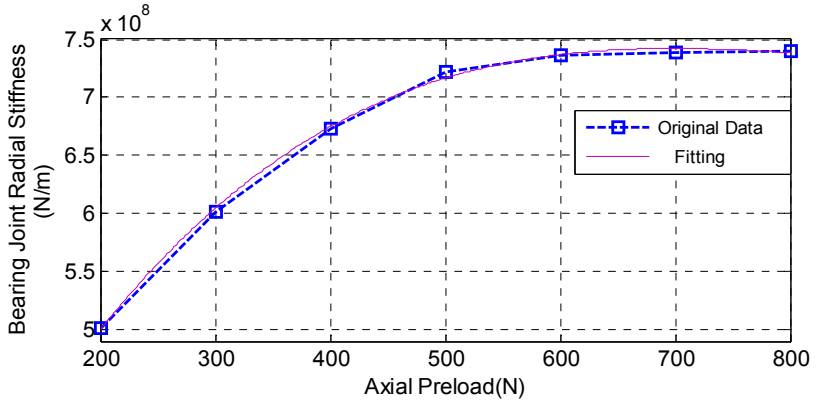

(a) The radial stiffness of bearing joint

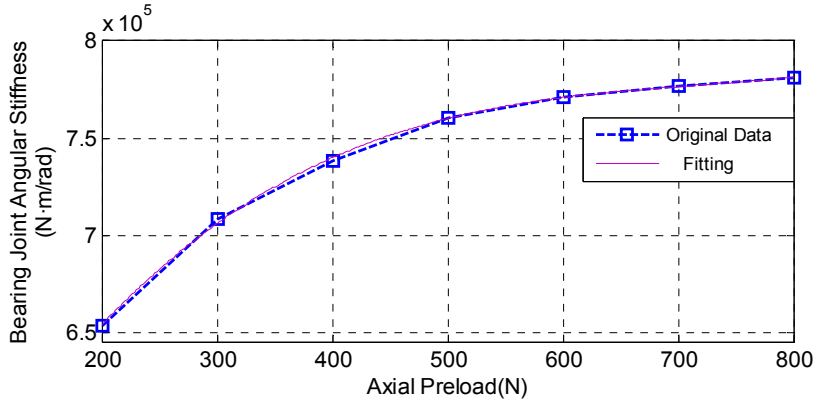

(b) The angular stiffness of bearing joint

Fig.13 The fitting curve of bearing joint stiffness

joint stiffness for the different spindle system by adopting the presented identification method of bearing joint.

4.2 The effect with and without bearing joint stiffness on the spindle system

According to the presented identification method, we can obtain the bearing joint stiffness under different preloads. For the purpose of comparing the dynamic characteristics of spindle system with and without the bearing joint stiffness, the simulation model is built in the ANSYS software, and the stiffness is assigned to the Matrix27 elements in the FE model as depicted in Section 3. Fig. 14 shows the frequency response diagram of spindle system with and without bearing joint stiffness under the preload 500N. Comparing with the bearing stiffness as the support stiffness of spindle system, the nature frequencies decrease when the bearing joint stiffness is considered in the FE model. The variation ratio is 0.12%, 6% and 14% for the 1st order to 3rd order nature frequencies of spindle system, respectively. The results show that the higher order mode of spindle system is obviously affected by the bearing joint. From the analysis results, we can conclude that the bearing joint can seriously affect the dynamic characteristics of spindle system. It is necessary to consider the bearing joint stiffness for improving the accuracy of

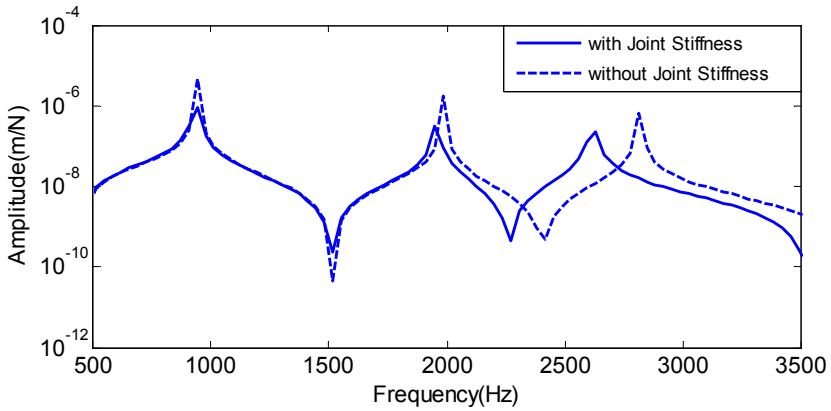

Fig. 14 The nature frequencies of spindle system with and without bearing joint stiffness

analysis. A proper assembly relationship and preload of bearing group are also the key factors for the high speed spindle system. The presented identification method can obtain the bearing joint stiffness, and give a quantified relationship of bearing joint and preload in a certain assembly relationship, which will help the designer to optimize the spindle system.

5. Conclusions

In this work, a hybrid identification method is presented to achieve the dynamic stiffness of bearing joint for the high speed spindles. The experimental set-up with variable preload spindle is developed to verify the validity of the presented identification method. The effect law of preload on the bearing joint stiffness is achieved and a fitting polynomial formula is set up to obtain the stiffness of bearing joint under different preloads rapidly. Comparing the FE model with and without bearing joint stiffness, the higher order mode of spindle system is obviously affected by the bearing joint. Therefore, it is crucial to identify the bearing joint stiffness and obtain the accurate analysis model of high speed spindle system.

Acknowledgments

This work was supported by Beijing Natural Science Foundation (No. 3132004) and National Natural Science Foundation of China (No. 51375025).

References

Altintas, Y. and Cao, Y.Z. (2005), "Virtual design and optimization of machine tool spindles", *CIRP Ann. Manuf. Tech.*, **54** (1), 379-382.

Aydin, G., Jason, T.D. and Singh, R. (2012), "Effect of bearing preloads on the modal characteristics of a shaft-bearing assembly: Experiments on double row angular contact ball bearings", *Mech. Syst. Signal Pr.*, **31**, 176-195.

Cao, Y.Z. and Altintas, Y. (2004), "A general method for the modeling of spindle-bearing systems", *ASME J. Mech. Des.*, **126** (6), 1089-1104.
Cao, Y.Z. and Altintas, Y. (2007), "Modeling of spindle-bearing and machine tool systems for virtual simulation of milling operations", *Int. J. Mach. Tool. Manuf.*, **47** (9), 1342-1350.
Čelič, D. and Boltežar, M. (2009), "The influence of the coordinate reduction on the identification of the joint dynamic properties", *Mech. Syst. Signal Pr.*, **23**(4), 1260-1271.
Chen, J.S. and Chen, K.W. (2005), "Bearing load analysis and control of a motorized high speed spindle", *Int. J. Mach. Tool. Manuf.*, **45**(12-13), 1487-1493.
DeMul, J.M., Vree, J.M. and Mass, D.A. (1989), "Equilibrium and association load distribution in ball and roller bearings loaded in five degrees of freedom while neglecting friction, Part I: General theory and application to ball bearings", *ASME J. Tribology*, **111** (1), 142-148.
Guo, Y. and Robert, G.P. (2012), "Stiffness matrix calculation of rolling element bearings using a finite element / contact mechanics model", *Mech. Mach. Theory*, **51**, 32-45.
Hagiu, G.D. and Gafitanu, M.D. (1992), "Dynamic characteristics of high speed angular contact ball bearings", *Wear*, **211**(1), 22-29.
Hamid, A. and Mostafa, N. (2010), "Tool point dynamics prediction by a three-component model utilizing distributed joint interfaces", *Int. J. Mach. Tool. Manuf.*, **50**(11), 998-1005.
Hernot, X., Sartor, M. and Guillot, J. (2000), "Calculation of the stiffness matrix of angular contact ball bearings by using the analytical approach", *Tran. ASME*, **122**(3), 83-90.
Hu, F., Wu, B., Hu, Y. and Shi, T. (2009), "Identification of dynamic stiffness matrix of bearing joint region", *Front. Mech. Eng. China*, **4**(3), 289-299.
Houpert, L. (1997), "A uniform analytical approach for ball and roller bearings calculations", *ASME J. Tribology*, **119**(4), 851-858.
Jalali, H., Ahmadian, H. and Mottershead, J.E. (2007), "Identification of nonlinear bolted lap-joint parameters by force-state mapping", *Int. J. Solid. Struct.*, **44**(25-26), 8087-8105.
Jeng, Y.R. and Gao, C.C. (2001), "Investigation of the ball-bearing temperature rise under an oil-air lubrication system", *Proc. Inst. Mech. Eng. Part J: J. Eng. Tribology*, **215**(2), 139-148.
Jiang, S.Y. and Mao, H.B. (2010), "Investigation of variable optimum preload for a machine tool spindle", *Int. J. Mach. Tool. Manuf.*, **50**(1), 19-28.
Jones, A.B. (1960), "A general theory for elastically constrained ball and radial roller bearings under arbitrary load and speed conditions", *ASME J. Basic Eng.*, **82**(2), 309-320.
Kashani, H. and Nobari, A.S. (2010), "Identification of dynamic characteristics of nonlinear joint based on the optimum equivalent linear frequency response function", *J. Sound Vib.*, **329**(9), 1460-1479.
Kim, S.M. and Lee, S.K. (2001), "Prediction of thermo-elastic behavior in a spindle bearing system considering bearing surroundings", *Int. J. Mach. Tool. Manuf.*, **41** (6), 809-831.
Kim, S.M., Lee, K.J. and Lee, S.K. (2002), "Effect of bearing support structure on the high-speed spindle bearing compliance", *Int. J. Mach. Tool. Manuf.*, **42** (3), 365-373.
Li, H.Q. and Shin, Y.C. (2004), "Analysis of bearing configuration effects on high speed spindles using an integrated dynamic thermo-mechanical spindle model", *Int. J. Mach. Tool. Manuf.*, **44**(4), 347-364.
Lim, T.C. and Singh, R. (1990), "Vibration transmission through rolling element bearings, Part I: Bearing stiffness formulation", *J. Sound Vib.*, **139**(2), 179-199.
Majid, M., Eldon, G. and Simon, S.P. (2013), "FRF based joint dynamics modeling and identification", *Mech. Syst. Signal Pr.*, **39**(1-2), 265-279.
Mao, K.M., Li, B., Wu, J. and Shao, X.Y. (2010), "Stiffness influential factors-based dynamic modeling and its parameter identification method of fixed joints in machine tools", *Int. J. Mach. Tool. Manuf.*, **50**(2), 156-164.
Michael, H., Stefan, O. and Lothar, G. (2002), "Identification of a bolted-joint model with fuzzy parameters loaded normal to the contact interface", *Mech. Res. Commun.*, **29**(2-3), 177-187.
Rivin, E.I. (2000), "Tooling structure: interface between cutting edge and machine tool", *Ann. CIPP*, **49**(2), 591-634.
Royston, T.J. (2008), "Leveraging the equivalence of hysteresis models from different fields for analysis and

numerical simulation of jointed structures", *J. Comput. Nonlin. Dyn.*, **3**, 1-8.
Schmitz, T.L. and Smith, K.S. (2009), *Machining Dynamics: Frequency Response to Improved Productivity,* Springer Science + Business Media, New York, NY, USA.
Shamine, D.M., Hong, S.W. and Shin, Y.C. (1998), "Experimental identification of dynamic parameters of rolling element bearings in machine tools", *J. Dyn. Syst. Measur. Control Tran.*, ASME, **122**(1), 95-101.
Yang, T.C., Fan, S.H. and Lin, C.S. (2003), "Joint stiffness identification using FRF measurements", *Comput. Struct.*, **81**(28-29), 2549-2556.

CC